



Contents lists available at ScienceDirect

Carbohydrate Research

journal homepage: www.elsevier.com/locate/carres

Chitosan as an active support for assembly of metal nanoparticles and application of the resultant bioconjugates in catalysis

Dongwei Wei^{a,†,*}, Yongzhong Ye^{a,†}, Xueping Jia^b, Chao Yuan^a, Weiping Qian^c

^a College of Life Science, Henan Agricultural University, Zhengzhou 450002, PR China

^b School of Chemistry and Chemical Engineering, Nantong University, Nantong 226007, PR China

^c State Key Laboratory of Bioelectronics, School of Biological Science and Medical Engineering, Southeast University, Nanjing 210096, PR China

ARTICLE INFO

Article history:

Received 23 July 2009

Received in revised form 11 October 2009

Accepted 13 October 2009

Available online 22 November 2009

Keywords:

Chitosan

Metal nanoparticles

Bioconjugates

Catalysis

ABSTRACT

Metal nanoparticle–chitosan (NPs–chitosan) bioconjugates were formed by exposure of chitosan to an aqueous solution of metal salts under thermal treatment. The metal nanoparticles that are formed strongly bound to chitosan, which encouraged us to investigate their catalytic performance. It was demonstrated that the metal NPs–chitosan bioconjugates functioned as effective catalysts for the reduction of 4-nitrophenol in the presence of NaBH₄, which was monitored by means of spectrophotometry as a function of reaction time. The silver NPs–chitosan bioconjugates exhibited excellent catalytic activity and were reusable for up to seven cycles. In contrast, the gold NPs–chitosan catalyst displayed poor catalytic activity, even in the second cycle. A highlight of our approach is that chitosan simultaneously acts as an active support for the synthesis and assembly of nanoparticles, and the resultant bioconjugates bear the advantage of easy separation from the reaction medium.

© 2009 Elsevier Ltd. All rights reserved.

1. Introduction

Much attention has been focused on the preparation of metal nanoparticles (especially gold and silver nanoparticles) because of their unusual properties compared to bulk metals and their important applications as antimicrobial agents, in catalysis, in optics, and as sensors.^{1–3} In particular, the preparation of metal nanoparticles immobilized on various matrices has attracted intensive research interest, because excellent synergy and bifunctional effects are expected.^{4–9} For instance, through spontaneous reduction of AuCl₄[−] ions by bis(2-(4-aminophenoxy)ethyl) ether at the liquid–liquid interface, gold nanoparticles were immobilized on this polymeric matrix, and thereafter were used as a support for pepsin.⁷ Recognizing the film-forming properties of chitosan, gold nanoparticles were immobilized in it, and the resultant gold–chitosan films were employed in trace analysis as surface-enhanced substrates (SERs) for Raman spectroscopy.⁸ Silver nanoparticles were spontaneously incorporated into poly(vinyl alcohol) film by thermal treatment, and the resultant materials were found to be promising candidates for optical limiting applications.³ The Sastry group reported the formation of gold nanoparticle–spider-silk bioconjugates by reaction of spider silk with aqueous chloroauric acid. In view of the contraction/expansion behavior of the fibers

in solvents of varying polarities, they demonstrated that exposure of the gold nanoparticle–spider-silk bioconjugates to vapors of methanol and chloroform led to changes in electrical transport through the nanoparticles, thus opening the possibility of developing a vapor sensor.⁹

There have been a large number of reports on the preparation of metal nanoparticles on matrix materials through various strategies such as thermal, electrochemical, photochemical, and sonochemical reduction.^{10–14} Although the preparation methods for metal nanoparticles are varied, the utilization of biomolecules for the synthesis of metal nanoparticles via the thermal reduction method is desirable for a mild and ecofriendly process.^{15–18} Chitosan, a polysaccharide biopolymer formed by the deacetylation of naturally occurring chitin, displays unique polycationic, chelating, and film-forming properties due to the presence of active amino and hydroxyl functional groups.¹⁹ With the development of environmentally friendly industries, chitosan and its derivatives, which combine nontoxicity, biocompatibility, biodegradability, and bioactivity with desirable physical and mechanical properties, are becoming increasingly important.^{20–25} In our recent work, we reported the preparation of gold nanoparticles by thermal and photochemical reduction methods in chitosan–acetic acid aqueous solution.^{13,26,27} Therein, we demonstrated that AuCl₄[−] ions could be reduced to zero-valent gold nanoparticles by chitosan itself without any additional reductant in thermal reduction.^{26,27} In our current work, we present a further study on the preparation of metal nanoparticle–chitosan (NPs–chitosan) bioconjugates by exposure of chitosan to an aqueous solution of metal salts under

* Corresponding author. Tel.: +86 371 63555790; fax: +86 371 63554528.

E-mail addresses: weidongwei@henau.edu.cn, weidongwei2008@gmail.com (D. Wei).

† These two authors contributed equally to this work.

thermal conditions. Significantly, the silver nanoparticles thus prepared were found to function as an effective catalyst for the reduction of 4-nitrophenol to 4-aminophenol, and they exhibited excellent catalytic activity and reusability for up to seven cycles. Nitrophenols and their derivatives, which result from the production processes of pesticides, herbicides, insecticides, and synthetic dyes, are some of the most refractory pollutants that can occur in industrial wastewaters. Now we are aware of the fact that water pollution by phenol and phenolic compounds is of great public concern.^{20,28} Therefore, this study also becomes much more fascinating from the point of pollution abatement. Besides, as there is a great demand for aromatic amino compounds in industry, the reaction becomes academically as well as technologically important. Also, it is worth noting that our current strategy for the synthesis of metal NPs–chitosan bioconjugates has some significant features: (1) nanoparticles are formed under mild and ecofriendly conditions in which chitosan simultaneously acts as both a reductant and scaffold for nanoparticles. (2) The resultant materials have the advantage of easy separation from the reaction medium, which present the possibility of their functioning as reusable catalysts. (3) Chitosan is nontoxic and biocompatible. Thus the metal NPs–chitosan bioconjugates formed are also very promising candidates for pharmaceutical and biomedical applications.

2. Experimental

2.1. Reagents

Chitosan flakes, from crab shells (Practical grade >85% deacetylated; Brookfield viscosity >200,000 cps) were purchased from Sigma–Aldrich. Sodium borohydride (NaBH_4), silver nitrate (AgNO_3) hydrogen tetrachloroaurate hydrate ($\text{HAuCl}_4 \cdot 3\text{H}_2\text{O}$), and 4-nitrophenol ($\text{C}_6\text{H}_5\text{NO}_3$) were of analytical grade. All compounds were used as received. All solutions were prepared with triply distilled water.

2.2. Instruments

The optical properties of the products were measured by a Shimadzu UV–vis–NIR spectrophotometer (UV-3150). Transmission electron microscopy (TEM) was carried out on a JEM-2000EX microscope at an accelerating voltage of 120.0 kV. Fourier-transform infrared spectroscopy (FTIR) was recorded on a Nicolet Nexus 870 FTIR instrument.

2.3. Formation of metal (gold or silver) nanoparticle–chitosan bioconjugates

The synthesis of metal (gold or silver) NPs–chitosan bioconjugates was carried out by exposure of chitosan flakes to an aqueous solution of metal salts ($\text{HAuCl}_4 \cdot 3\text{H}_2\text{O}$ or AgNO_3). In a typical procedure, 30 mg of chitosan flakes were added to a test tube with 1 mL of the designated concentration of metal salts solution and 6 mL of the triply distilled water at room temperature. The nanoparticle conjugate settled at the bottom of the tube after storage for 10 min, even without centrifugation. After the supernatant solution became colorless (about 30 min), the test tubes containing the above mixtures were heated to the selected temperature (between 45 and 95 °C) and left standing for about 12 h. Then, the resultant mixture was cooled and mixed for homogenization for UV–vis spectroscopy measurements. To confirm the binding of metal nanoparticles onto chitosan for subsequent catalytic reactions, the resultant mixtures containing metal NPs–chitosan bioconjugates were centrifuged and redispersed in triply distilled water at least four times. Thereafter, the bioconjugates were dried and used

as catalysts for the reduction of 4-nitrophenol. The parallel samples after centrifugation and redispersion were characterized by TEM and FTIR. All the reactions were carried out in aqueous solution at pH 5.9. To investigate the pH effect on the formation of metal NPs–chitosan bioconjugates, 1 M NaOH solution was used to adjust the pH of the medium.

2.4. Catalytic properties of metal NPs–chitosan bioconjugates for nitrophenol reduction

The reduction of 4-nitrophenol by NaBH_4 was studied as a model reaction to probe the catalytic activity of metal (gold or silver) NPs–chitosan bioconjugates in a heterogeneous system for 4-nitrophenol reduction. The catalytic reaction was carried out in a standard quartz cell with a 1-cm path length and ~3.2 mL volume. The procedures were as follows: 1 mL of 15 mM NaBH_4 was added to 2 mL of triply distilled water containing 2.0 mM 4-nitrophenol (120 μL) in a quartz cell. The color changed from light yellow to yellow-green. Immediately after the addition of metal NPs–chitosan bioconjugates, the absorption spectra were recorded in 1-min intervals in the range of 200–600 nm at room temperature (25 °C).

3. Results and discussion

3.1. Formation and characterization of metal NPs–chitosan bioconjugates

Figure 1 shows the representative photographs of metal NPs–chitosan bioconjugates formed by exposure of chitosan flakes to aqueous solution of metal salts under thermal treatment at designated parameters. It is clear from Figure 1 that when chitosan flakes are exposed to hydrochloroauric acid, the colorless chitosan (Fig. 1a) turns red (Fig. 1b–d). A characteristic surface plasmon resonance (SPR) band for gold nanoparticles suggests the formation of gold nanoparticles.²⁶ It is also apparent that there is a progressive increase in the red color with an increase of hydrochloroauric acid concentration, which is attributed to the increased content of gold nanoparticles. Furthermore, when chitosan flakes are exposed to silver nitrate, the silver NPs–chitosan samples formed exhibited a yellowish-brown or brown color, and a characteristic SPR band for silver nanoparticles (Fig. 1e–g).²⁷ Also, the color of the silver NPs–chitosan samples changed from yellow to brown with an increase in silver nitrate concentration, which is attributed to the increased amount of silver nanoparticles. Moreover, it is apparent that the color of the samples formed is different before and after the adjustment of the pH of the medium (compared Fig. 1e–g with Fig. 1h–j). It is known that the SPR band for nanoparticles is sensitive to the size, shape, and spatial distribution of the particles.¹⁶ Hence, the difference in the color of the silver samples suggest the pH of the medium has an effect on the interaction of chitosan with silver nitrate, and accordingly, the characteristics of silver nanoparticles, since the color of metal nanoparticles is related to the SPR excitation.

Figure 2a shows the optical spectra of the metal NPs–chitosan bioconjugates by exposure of chitosan flakes to triply distilled water, hydrochloroauric acid, and silver nitrate, respectively, at 95 °C. It is evident from Figure 2a that the sample from the exposure of chitosan flakes to triply distilled water exhibits no absorption band, and the samples from the exposure to hydrochloroauric acid or silver nitrate show their corresponding characteristic SPR bands, further demonstrating that the color of NPs–chitosan samples originate from the metal nanoparticles that are formed in the chitosan matrix.²⁶ Figure 2b compares the optical spectra of the samples formed in the presence and absence of chitosan. It is clear from Figure 2b that the samples formed in the presence of chitosan show the characteristic SPR band for metal nanoparticles

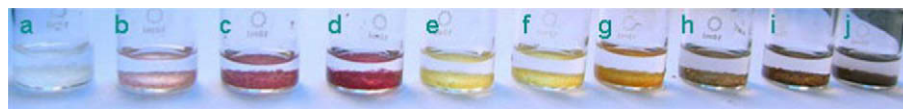


Figure 1. Formation of metal NPs–chitosan bioconjugates by exposure of 30 mg of chitosan flakes at 95 °C to (a) triply distilled water, (b) 0.2, (c) 0.5, (d) 1.0 mM HAuCl_4 , (e) 1.0, (f) 3.0, (g) 6.0 mM AgNO_3 , (h) 6.0, (i) 6.0, and (j) 12.0 mM of AgNO_3 . Therein, (a–g) pH 5.9, (h) pH 7.0, and (i and j) pH 9.0.

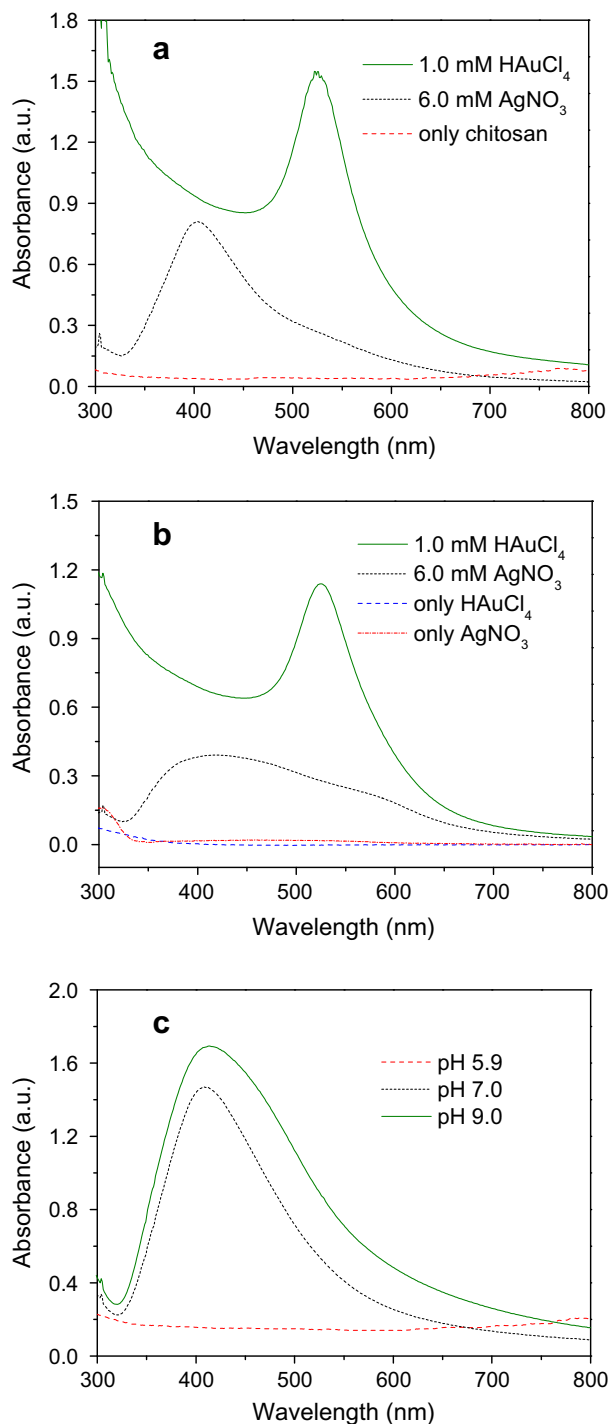


Figure 2. UV–vis spectra of samples obtained under different reactive parameters (as indicated on each plate): (a) 95 °C, (b) 80 °C, (c) 45 °C and 6.0 mM AgNO_3 .

centered at about 530 nm (gold nanoparticles) or 420 nm (silver nanoparticles).²⁷ The samples formed in the absence of chitosan,

nevertheless, show no absorption band in the UV–vis region. Also, no color change in the medium solution was observed during the reaction process when chitosan is absent, suggesting the reduction of metal salts did not occur. Therefore, it is concluded that chitosan acts as a reductant for the formation of metal nanoparticles, and when chitosan is absent, the reduction of metal salts cannot be realized. Moreover, we also studied system with exposure of chitosan to metal salt solution at pH 5.9, 7.0, and 9.0, respectively, as shown in Figure 2c. It is apparent from Figure 2c that at pH 5.9 (triply distilled water), no absorption band is observed, even from exposure of chitosan to silver nitrate for 12 h at 45 °C. Also no color change in solution was observed. However, the solution color quickly changed from colorless to bright yellow when the pH of the medium was adjusted to 7.0 or 9.0 by 1 M sodium hydroxide solution, and concomitantly the characteristic absorption band of silver nanoparticles appeared. The above experimental results demonstrate that the pH of the medium affects the reduction of silver nitrate salts by chitosan. The reason may be that the redox potential of the silver nitrate salts is related to the pH of the medium: the pH elevation favors the hydrolyzation (hydrolysis) of silver ions, and, therefore, the formation of Ag_2O , which advantageously accelerates the reduction of silver nitrate by chitosan. In contrast, the pH elevation disfavored the hydrolyzation (hydrolysis) of hydrochloroauric acid salts by the increase in the number of hydroxyl radicals and, accordingly, slowed down the reduction of hydrochloroauric acid salts by chitosan. As a result, the reduction of hydrochloroauric acid salts by chitosan did not occur even when incubated for 12 h at 45 °C at pH 5.9, 7.0, and 9.0. A detailed discussion of the mechanism is presented below.

TEM images and the electron diffraction pattern further confirmed the formation of metal NPs–chitosan bioconjugates as demonstrated in Figure 3. It is evident from Figure 3 that metal nanoparticles were formed in the chitosan matrix, whereas there are some differences in nanoparticle size and size distribution under the different reaction parameters (compare Fig. 3a–c and Fig. 3b–d, respectively). Furthermore, it is clear that when the pH of the medium was adjusted, the size distribution of silver nanoparticles was altered, which is in accord with the corresponding illustration in Figure 1e–j. The electron diffraction pattern collected during TEM images further revealed the formation of gold (Fig. 3c) or silver (Fig. 3f) nanoparticles in the chitosan matrix.²⁷

The formation of metal NPs–chitosan bioconjugates was further confirmed by FTIR measurements. Figure 4 shows the FTIR spectra of the chitosan and NPs–chitosan samples. It is clear from Figure 4 that, although there is the possibility of overlapping between the N–H and the O–H stretching vibrations, the strong broad band at 3300–3500 cm^{-1} is characteristic of the N–H stretching vibration.²⁹ The gradual blue shift of transmittance in this band region with the increased silver concentration indicates that the N–H vibration was affected by the attachment of silver. The attachment of silver to nitrogen atoms in the chitosan molecules reduced the vibration intensity of the N–H bond due to the increase in molecular weight with silver binding. Our results are consistent with that of Panigrahi et al. who suggested that the N–H stretching at 3447 cm^{-1} , which is attributed to the C– NH_3 on pure resin particles, shows a blue shift after immobilization of the gold particles onto the resin beads because of the new Au–N bond formation.²⁸

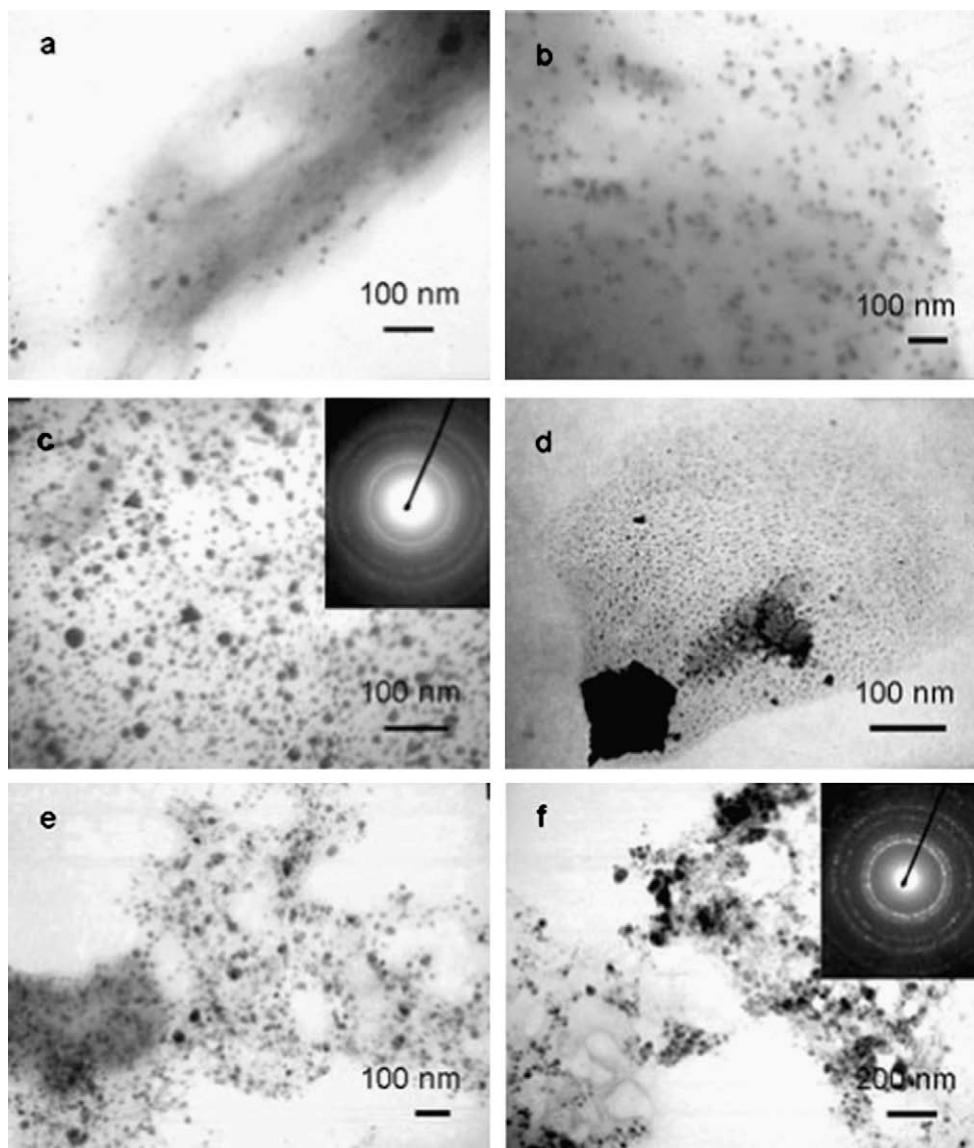


Figure 3. TEM images of metal NPs–chitosan bioconjugates by exposure of 30 mg of chitosan flakes to (a) 1.0 mM HAuCl₄ at 95 °C, (b) 6.0 mM AgNO₃ at 95 °C, (c) 1.0 mM HAuCl₄ at 80 °C, (d) 12.0 mM AgNO₃ at 80 °C, (e) 6.0 mM AgNO₃ at 45 °C, and (f) 6.0 mM AgNO₃ at 45 °C. Therein, (a–d) pH 5.9, (e) pH 7.0, and (f) pH 9.0.

Moreover, it is noted that metal NPs–chitosan samples (Fig. 4e–h) show a new band at about 1740 cm⁻¹ that corresponds to the carbonyl stretch vibrations in ketones, aldehydes and carboxylic acids. The presence of the 1740 cm⁻¹ signal in the metal NPs–chitosan samples indicates that the reduction of the silver ions is coupled to the oxidation of the hydroxyl groups in the chitosan molecules and/or their hydrolyzates,²⁷ but this signal was obviously not observed when the metal salt concentrations were low enough. Hence, Figure 4 gives sound evidence that gold or silver nanoparticles are strongly bound to the chitosan matrix.

3.2. Proposed mechanism for the formation of metal NPs–chitosan bioconjugates

Mills and co-workers³⁰ and Liu and co-workers³¹ have investigated the reduction of silver ions in alcoholic solutions. They demonstrated that Ag⁺ ions could be reduced and form metal particles; meanwhile, the alcohol molecules were transformed into their corresponding aldehydes and acids. According to the previous reports and our experimental results, the mechanism for the formation of

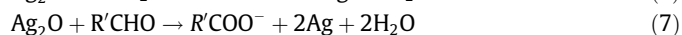
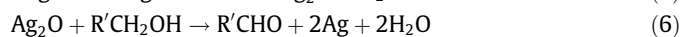
silver NPs–chitosan bioconjugates should be represented by the following reactions.

Step A: The adsorption of silver ions onto chitosan.



where R represents all other components except –NH₂ in chitosan.

Step B: The formation of silver NPs–chitosan bioconjugates.



where R' represents all other components except –CH₂OH in chitosan.

It is mentioned above that the amine groups in chitosan molecules have strong complexation abilities with metal ions, and,

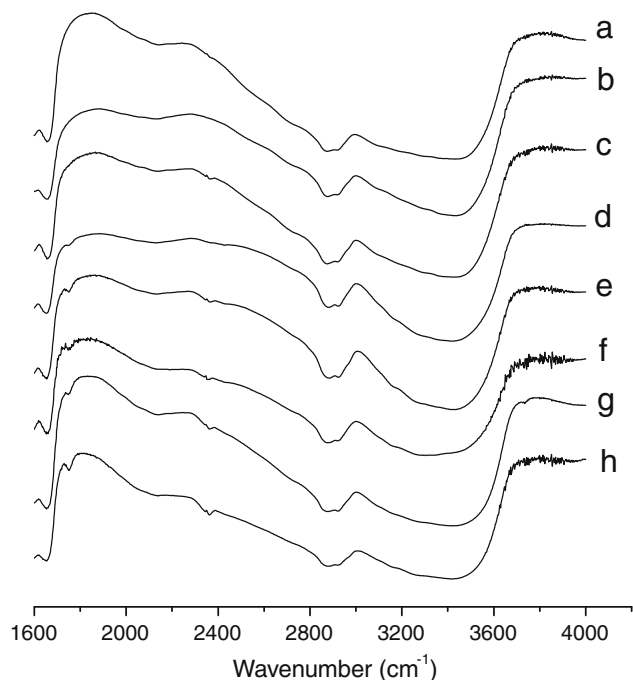
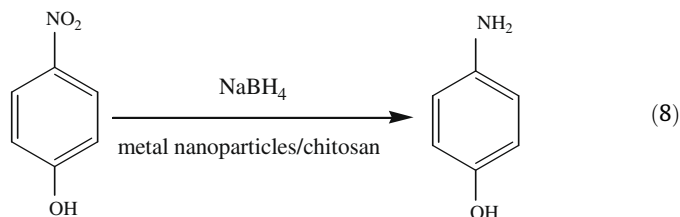


Figure 4. FTIR spectra of the metal NPs–chitosan bioconjugates prepared by exposure of 30 mg of chitosan flakes to (a) triply distilled water, (b) 1.0 mM H₂AuCl₄, (c) 3.0 mM, (d) 6.0 mM, (e) 12.0 mM, (f) 6.0 mM, (g) 6.0 mM, and (h) 12.0 mM AgNO₃. Therein, (a–e) pH 5.9, (f) pH 7.0, (g and h) pH 9.0.

therefore, chitosan has been investigated as an absorption material for recovering heavy metal ions from industrial effluents.^{23,28} For the equations shown above, the two initial steps are the binding of silver ions to the amine groups in chitosan molecules due to the sharing of lone electron pairs from the nitrogen atom in chitosan with silver ion (Eq. 1) and a competitive adsorption of Ag⁺ over H⁺ to the nitrogen atom (Eq. 2). In addition, the complexes of R–NH₂Ag⁺ are subject to the reaction in Eq. 3 due to the greater binding force of Ag ions with the OH[−] group from water than with the nitrogen of the amino group. Thus, a two-step process is considered for the formation of silver nanoparticles in the chitosan matrix, viz., the formation of silver NPs–chitosan bioconjugates: First, silver ions are diffused onto the surface of chitosan molecules and interacted with OH[−] to form Ag₂O particles (Eq. 4). Second, the Ag₂O particles are reduced by chitosan and adsorbed on to chitosan. At the same time, the chitosan –OH group are oxidized to their corresponding aldehydes and acids (Eqs. 5 and 6).

The formation of gold NPs–chitosan bioconjugates also took place in two steps, viz., the adsorption of gold ions onto chitosan and the subsequent reduction of gold species by chitosan. Nevertheless, the pH of the medium has distinct influences on the reduction of two kinds of metal precursors. For the reduction of silver salts, the reaction is shifted toward the formation of Ag₂O (Eq. 5) with the increasing pH of the medium, viz., the increasing hydroxide ion concentration. Accordingly, the increased Ag₂O concentration favors the reduction of the silver species by chitosan (Eqs. 6 and 7). Hence, the elevation of the pH of the medium accelerates the reduction of silver nitrate with chitosan. On the other hand, for the interaction of hydrochloroauric acid with chitosan, increasing pH of the medium, viz., the increasing hydroxide ion concentration disfavors the hydrolyzation of AuCl₄[−], and, consequently, the formation of Au³⁺,³² thus slowing down the reduction of hydrochloroauric acid with chitosan. Therefore, the elevation of the pH of the medium did not facilitate the reduction of hydrochloroauric acid with chitosan.

3.3. Catalytic properties of metal NPs–chitosan bioconjugates for 4-nitrophenol reduction



Chitosan has been extensively used as a support for catalysis during the past few decades.^{20,21,33} One of the important applications of metal nanoparticles is to activate/catalyze some reactions that are otherwise unfeasible.^{28,34,35} To this end, the catalytic function of metal NPs–chitosan bioconjugates on the reduction of 4-nitrophenol as a model reaction was investigated in the study. It was observed that the UV absorption peak of 4-nitrophenol underwent a red shift from 317 to 400 nm (due to the generation of 4-nitrophenolate ions)³⁶ immediately upon the addition of an aqueous solution of NaBH₄. At the same time, there is a significant change in solution color from light yellow to yellow-green. The absorption peak at 400 nm remained unaltered for a long duration when a metal NPs–chitosan was absent, demonstrating the reduction of 4-nitrophenolate ions could not be realized with only the strong reducing agent NaBH₄.³⁶ Herein we first demonstrate the reduction of 4-nitrophenol in the presence of silver–chitosan catalyst. Figure 5 shows the UV–vis spectra for the reduction of 4-nitrophenol with the addition of silver–chitosan samples measured at 1-min intervals during the reaction. It is evident from Figure 5 that, as the absorption band of 4-nitrophenolate ions centered at 400 nm decreases and disappears, and two new peaks at 300 nm and 230 nm appear, which are attributed to the generation of 4-aminophenol³⁷ as represented in Eq. 8. Concomitantly, evolution of small bubbles of hydrogen gas surrounding the catalyst particles helps to stir the solution. As a result, the catalyst particles remain well distributed in the reaction mixture during the progress of the reaction and offer favorable conditions for a smooth reaction. Interestingly, upon the addition of metal NPs–chitosan samples, the reaction solution caused a fading and ultimate bleaching of the yellow-green color derived from 4-nitrophenolate ions, suggesting the occurrence of a reduction reaction. To exclude the possibility that the reduction reaction might be activated by chitosan

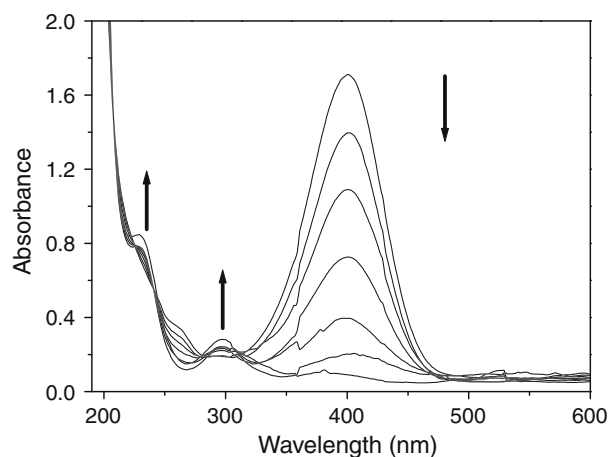


Figure 5. UV–vis absorption spectra for reduction of 4-nitrophenol measured at 1-min intervals by the silver NPs–chitosan catalyst for exposure of 30 mg of chitosan flakes to 6.0 mM AgNO₃ (95 °C) as catalyst in the third cycle.

instead of the silver NPs–chitosan samples, chitosan alone was added into the aqueous solution of 4-nitrophenol and NaBH_4 mixture. It was found that no change in the color and position of the absorption band at 400 nm of 4-nitrophenolate ions was observed, which suggests that the reduction of 4-nitrophenol did not proceed when silver NPs–chitosan samples were absent.³⁶ Thus, the reduction of 4-nitrophenol by NaBH_4 has been clearly demonstrated to be activated by silver NPs–chitosan as catalyst. In our system, the silver particles start the catalytic reduction by relaying electrons from the donor BH_4^- to the acceptor 4-nitrophenol right after their adsorption onto the catalyst particle surface. A detailed discussion is presented below.

In industrial applications, catalysis may be performed in homogeneous systems. However, in the case of expensive catalysts such as those involving precious and strategic metals, it is important to recover the metal catalysts at the end of the process.^{21,28,38} Therefore, we prepared the above mixtures by centrifuging and redispersing them in triply distilled water at least four times for subsequent reuse experiments. As shown in Figure 6, the catalytic activities for reuse are estimated by the translation time of 95% 4-nitrophenol. It is evident from Figure 6 that the silver NPs–chitosan samples are not only very effective for the catalytic reduction of aromatic nitro compounds, but also are recoverable and can be recycled a number of times. Figure 6 shows the representative results of the silver NPs–chitosan samples as catalysts for seven successive cycles. It is clear from Figure 6 that the translation time of 95% 4-nitrophenol is 5 min for the first cycle, and for the 3rd and 5th reuse cycles, the translation time is 7 min and 11 min, respectively. Moreover, the translation time of 95% 4-nitrophenol is 2.6 times (13 min) of the initial time (5 min) during the 7th reuse cycle. Hence, above results clearly underline the fact that, although the catalytic activity of the silver NPs–chitosan samples gradually falls off during the recycles, the reduction of 4-nitrophenol by NaBH_4 could also be done fast for the 7th reuse cycle compared to the system in which a catalyst is absent, viz, silver NPs–chitosan samples as the catalyst possess remarkable reuse characteristics. As demonstrated in the Experimental (Section 2.3), the loss of silver nanoparticles during the reuse cycle is not observed or measured by UV–vis spectrometry. Thus, the decrease in catalyst

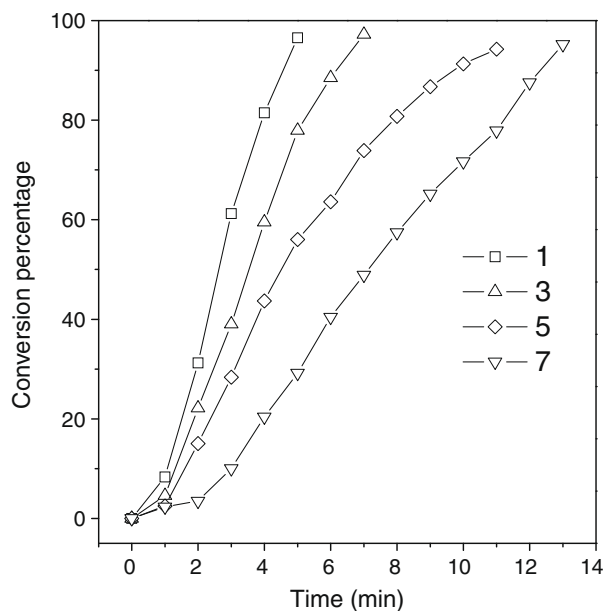


Figure 6. Conversion–time plot for reduction of 95% 4-nitrophenol by the silver NPs–chitosan catalyst for exposure of 30 mg of chitosan flakes to 6.0 mM AgNO_3 at 95 °C as a function of time during the reuse cycles.

activity during the successive reuse cycles may be attributed to the deactivation of active sites on the silver catalyst surface due to the increasing absorbent.

The activity of gold NPs–chitosan samples as a catalyst for the reduction of 4-nitrophenol by NaBH_4 was also investigated. Similar results were observed for the gold NPs–chitosan samples, and the results are shown in Figure 7. It is clear from Figure 7 that upon the addition of gold NPs–chitosan samples to the reaction system, the peak height at 400 nm attributed to 4-nitrophenolate ions gradually decreases with time. With the gradual decrease in peak height at 400 nm, a new peak appeared at 295 nm, indicating the formation of 4-aminophenol.³⁶ At the same time, a fading and ultimate bleaching of the yellow–green color in the aqueous solution and evolution of small bubbles of hydrogen gas surrounding the catalyst particles were observed when the gold NPs–chitosan sample was added to the reaction system, indicating the reduction of 4-nitrophenol and the formation of 4-aminophenol.³⁷ In another experiment, we found that the translation time from 4-nitrophenol to 4-aminophenol with the addition of gold NPs–chitosan samples prepared for 1 h is much shorter for the gold NPs–chitosan samples prepared for 12 h, as is illustrated in Figure 7 (compare Fig. 7a and b). That is to say, the catalytic activity of gold NPs–chitosan samples prepared for 1 h is much higher than that of the gold NPs–chitosan samples prepared for 12 h. The distinctive difference in the activity of these two particle samples prepared under different reaction times may be that the gold nanoparticles in the chitosan samples prepared for 1 h are still growing, and the samples are

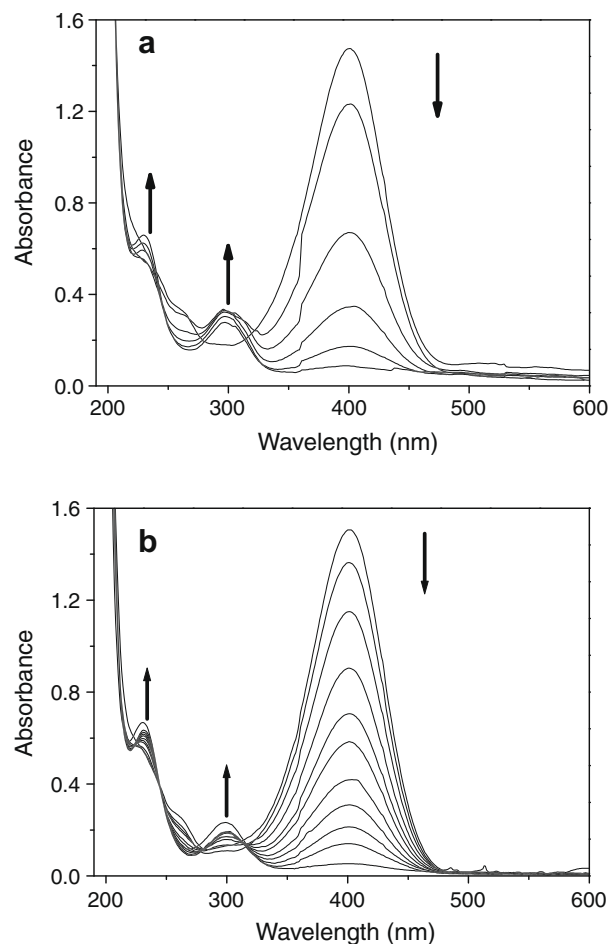


Figure 7. UV–vis absorption spectra for reduction of 4-nitrophenol measured at 1-min intervals by the gold NPs–chitosan catalyst for exposure of 30 mg of chitosan flakes to 1.0 mM gold precursors with chitosan (a) for 1 h and (b) for 12 h at 95 °C.

made up of smaller particles. Smaller particles are composed of a higher fraction of coordinatively unsaturated surface atoms, which increases the surface roughness and promotes the chemisorption of the 4-nitrophenolate ions and thereby facilitates the reaction. While gold nanoparticles prepared for 12 h are fully grown, the surfaces of the larger gold particles are terminated primarily by low-index, high-coordination surfaces related to the lower surface roughness. The lower surface roughness is unfavorable for the chemisorption of the nitrophenolate ions and thereby does not facilitate the reaction. In fact, the UV–vis observation for the formation of gold nanoparticles did reveal that the absorption peak of gold NPs–chitosan samples prepared for 1 h was increasingly strengthening, and that the absorption peak of samples prepared for 12 h was steady, which also was confirmed by their color development during the formation process of the gold NPs–chitosan samples. In the recent past, it has been reported by the Pal group that, for some redox reactions, the rate of catalysis involving the growing metal nanoparticles was higher than that involving fully grown nanoparticles,^{37,39} which is in accord with our results. Furthermore, other experimental results revealed that the silver NPs–chitosan samples as catalyst follow the same law for this reduction reaction, that is, the catalytic activity involving the silver NPs–chitosan samples prepared for 1 h was higher than that involving silver NPs–chitosan samples prepared for 12 h. It is also worthwhile to mention that when the silver NPs–chitosan samples prepared from high silver concentrations acted as a catalyst, the reduction of 4-nitrophenol could be done quickly, and the transition from 4-nitrophenol to 4-aminophenol could not be measured by a UV–vis spectrometer.

The reusable activity of gold NPs–chitosan samples as catalysts was explored. After the first cycle, the gold NPs–chitosan samples were centrifuged and redispersed in triply distilled water at least four times for subsequent reuse. It was found the gold NPs–chitosan samples thus prepared displayed poor catalytic activity even in the second cycle. The reduction from 4-nitrophenol to 4-aminophenol could not be achieved even with gold NPs–chitosan samples that were prepared for 1 h as the catalyst. The reason may be that the catalytic activity of a catalyst is related to the active sites in its surface, and gold NPs–chitosan samples easily absorb the reactant or product, thus making them poisoned with loss of activity. Therefore, even smaller particles with a higher activity of unsaturated surface atoms available for catalytic activity also deactivate in the second reuse. Additionally, the loss of the catalytic activity for the metal NPs–chitosan samples are also related to the interactions between chitosan and the metal species, since the diffusion of reactants onto the chitosan matrices is influenced by the network and the charge of chitosan. Further investigations are required to fully understand the exact reasons.

In our experiment, we did not estimate the metal loading in the metal NPs–chitosan bioconjugates. The depth of color for the metal NPs–chitosan samples increased with the increased metal salt concentrations, which in general indicates the increased metal loading, as shown in Figure 1. In our experimental work, we investigated the catalytic activities of variable amounts catalyst for the reduction of 4-nitrophenol by NaBH₄. It was demonstrated that, with increased metal salt concentrations, viz., increased catalyst loading, the transition from 95% 4-nitrophenol to 4-aminophenol was faster, while the other parameters remained constant. These results are consistent with the results from the Panigrahi group that showed the catalytic behavior of the gold nanoparticles for the reduction of the aromatic nitro compounds. The reaction rate was elevated with increased catalyst loading.²⁸

Furthermore, attention must be paid to the fact that a delay time t_0 was found for the catalytic reduction in all the cases, which may be due to the activation of the catalyst in the reaction mixtures. A similar behavior has been observed by other groups as well for this cat-

alytic reaction by metal nanoparticles.^{36–39} Pradhan et al. reported that the delay time t_0 for the reduction of aromatic nitro compounds in an oxygen atmosphere is greater than in a nitrogen atmosphere where it is smaller and negligible, in comparison to that for ambient conditions.³⁷ In the present case, the positive charge of the chitosan matrix activates the negatively charged 4-nitrophenolate and borohydride ions for adsorption and therefore facilitates the electron transfer from BH₄⁻ (donor) ion to the nitrophenolate (acceptor) ion through the metal surface. As soon as NaBH₄ is added, the metal particles start the catalytic reduction by relaying electrons from the donor BH₄⁻ to the acceptor 4-aminophenol right after their adsorption onto the catalyst particle surface. Moreover, evolution of small bubbles of hydrogen gas surrounding catalyst particles is essential for stirring the solution. Accordingly, the catalyst particles remain well distributed in the reaction mixture and offer favorable conditions for the reaction to occur smoothly. As NaBH₄ was present in large excess, its consumption for the reduction of oxygen did not alter its concentration noticeably. The induction period observed in the initial stages of the reaction is different as the particle properties are varied.

4. Conclusions

In this study, we have shown the feasibility of our route to form metal NPs–chitosan bioconjugates by exposure of chitosan to an aqueous solution of metal salts in which chitosan simultaneously acts as a reductant and scaffold for the formation of nanoparticles. Compared to the traditional chemical reduction approach, our method for the formation of metal NPs–chitosan bioconjugates is in agreement with the ‘green’ requirement nowadays. Also, the catalytic function of the resultant bioconjugates to activate the reduction of aromatic nitro compounds in the presence of NaBH₄ has been clearly confirmed by both visual observation and UV–vis spectra. It was demonstrated that silver NPs–chitosan bioconjugates exhibited excellent reuse characteristics over seven successive reaction cycles. However, the gold nanoparticles as prepared are only effective for the first cycle and are deactivated in the second cycle. It is also significant to explore the pharmaceutical and biomedical applications of metal NPs–chitosan bioconjugates in view of the unusual properties of metal nanoparticles and the biocompatible characteristics of chitosan.

References

1. Zeng, F.; Hou, C.; Wu, S. Z.; Liu, X. X.; Tong, Z.; Yu, S. N. *Nanotechnology* **2007**, *18*, 055605 (8pp).
2. Porel, S.; Singh, S.; Harsha, S. S.; Rao, D. N.; Radhakrishnan, T. P. *Chem. Mater.* **2005**, *17*, 9–12.
3. Ding, S. H.; Qian, W. P.; Tan, Y.; Wang, Y. *Langmuir* **2006**, *22*, 7105–7108.
4. Manna, S.; Batabyal, S. K.; Nandi, A. K. *J. Phys. Chem. B* **2006**, *110*, 12318–12326.
5. Esumi, K.; Isono, R.; Yoshimura, T. *Langmuir* **2004**, *20*, 237–243.
6. Dotzauer, D. M.; Bhattacharjee, S.; Wen, Y.; Bruening, M. L. *Langmuir* **2009**, *25*, 1865–1871.
7. Phadtare, S.; Vinod, S. P.; Wadgaonkar, P. P.; Rao, M.; Sastry, M. *Langmuir* **2004**, *20*, 3717–3723.
8. Dos Santos, D. S.; Goulet, P. J. G.; Pieczonka, N. P. W.; Oliverira, O. N.; Aroca, R. F. *Langmuir* **2004**, *20*, 10273–10277.
9. Singh, A.; Hede, S.; Sastry, M. *Small* **2007**, *3*, 466–473.
10. Huang, H. Z.; Yang, X. R. *Carbohydr. Res.* **2004**, *339*, 2627–2631.
11. Vigneshwaran, N.; Nachane, R. P.; Balasubramanya, R. H.; Varadarajan, P. V. *Carbohydr. Res.* **2006**, *34*, 2012–2018.
12. Okitsu, K.; Mizukoshi, Y.; Yamamoto, T. A.; Maeda, Y.; Nagata, Y. *Mater. Lett.* **2007**, *61*, 3429–3431.
13. Wei, D. W.; Qian, W. P. *J. Nanosci. Nanotechnol.* **2006**, *6*, 2508–2514.
14. Hoppe, C. E.; Lazzari, M.; Pardiñas-Blanco, I.; López-Quintela, M. A. *Langmuir* **2006**, *22*, 7027–7034.
15. Huang, H. Z.; Yang, X. R. *Biomacromolecules* **2004**, *5*, 2340–2346.
16. Wei, D. W.; Qian, W. P.; Shi, Y.; Ding, S. H.; Xia, Y. *Carbohydr. Res.* **2008**, *343*, 512–520.
17. Wu, L. L.; Shi, C. S.; Tian, L. F.; Zhu, J. J. *Phys. Chem. C* **2008**, *112*, 319–323.
18. Wang, B.; Chen, K.; Jiang, S.; Reincke, F.; Tong, W.; Wang, D.; Gao, C. Y. *Biomacromolecules* **2006**, *7*, 1203–1209.

19. Yi, H.; Wu, L. Q.; Bentley, W. E.; Ghodssi, R.; Rubloff, G. W.; Culver, J. N.; Payne, G. F. *Biomacromolecules* **2005**, *6*, 2881–2894.
20. Vincent, T.; Guibal, E. *Langmuir* **2003**, *19*, 8475–8483.
21. Guibal, E. *Prog. Polym. Sci.* **2005**, *30*, 71–109.
22. Kyzas, G. Z.; Bikiaris, D. N.; Lazaridis, N. K. *Langmuir* **2008**, *24*, 4791–4799.
23. Liu, X. W.; Hu, Q. Y.; Fang, Z.; Zhang, X. J.; Zhang, B. B. *Langmuir* **2009**, *25*, 3–8.
24. Duan, W. G.; Shen, C. M.; Fang, H. X.; Li, G. H. *Carbohydr. Res.* **2009**, *344*, 9–13.
25. Jin, X. X.; Wang, J. T.; Bai, J. *Carbohydr. Res.* **2009**, *344*, 825–829.
26. Wei, D. W.; Qian, W. P.; Shi, Y.; Ding, S. H.; Xia, Y. *Carbohydr. Res.* **2007**, *342*, 2494–2499.
27. Wei, D. W.; Qian, W. P. *Colloids Surf., B* **2008**, *62*, 136–142.
28. Panigrahi, S.; Basu, S.; Praharaj, S.; Pande, S.; Jana, S.; Pal, A.; Ghosh, S. K.; Pal, T. *J. Phys. Chem. C* **2007**, *111*, 4596–4605.
29. Jin, L.; Bai, R. *Langmuir* **2002**, *18*, 9765–9770.
30. Huang, Z. Y.; Mills, G.; Hajek, B. J. *Phys. Chem.* **1993**, *97*, 11542–11550.
31. Jiang, Z. J.; Liu, C. Y.; Liu, Y. *Appl. Surf. Sci.* **2004**, *233*, 135–140.
32. Eustis, S.; Hsu, H. Y.; El-Saved, M. A. *J. Phys. Chem. B* **2005**, *109*, 4811–4815.
33. Jiang, Y. J.; Zhang, L.; Yang, D.; Li, L.; Zhang, Y. F.; Li, J.; Jiang, Z. Y. *Chem. Res.* **2008**, *47*, 2495–2501.
34. Merga, G.; Cass, L. C.; Chipman, D. M.; Meisel, D. J. *Am. Chem. Soc.* **2008**, *130*, 7067–7076.
35. Han, J.; Liu, Y.; Guo, R. *J. Am. Chem. Soc.* **2009**, *131*, 2060–2061.
36. Liu, J. C.; Qin, G. W.; Raveendran, P.; Ikushima, Y. *Chem. Eur. J.* **2006**, *12*, 2131–2138.
37. Pradhan, N.; Pal, A.; Pal, T. *Colloids Surf., A* **2002**, *196*, 247–257.
38. Mei, Y.; Sharma, G.; Lu, Y.; Ballauff, M. *Langmuir* **2005**, *21*, 12229–12234.
39. Jana, N. R.; Sau, T. K.; Pal, T. *J. Phys. Chem. B* **1999**, *103*, 115–121.